

LA-UR-04-0006

Shock Compression of Deuterium and the Interiors of Jupiter and Saturn

D. Saumon¹

Los Alamos National Laboratory, MS F699, Los Alamos, NM 87545, USA

dsauomon@lanl.gov

and

T. Guillot

Observatoire de la Côte d'Azur, BP 4229, 06304 Nice CEDEX 04, FRANCE

guillot@obs-nice.fr

ABSTRACT

Recently, deuterium has been the focus of a high level of experimental and theoretical activity that was sparked by a disagreement on the experimental value of the maximum compression along the Hugoniot. The behavior of deuterium at Mbar pressures is not well understood.

It is of great interest to understand how the current uncertainty on the hydrogen/deuterium EOS affects the inferred structures of Jupiter and Saturn. In particular, the mass of a core of heavy elements (other than H and He) and the total mass of those heavy elements in these two planets are quite sensitive to the EOS of hydrogen and constitute important clues to their formation process. We present a study of the range of structures allowed for Jupiter and Saturn by the current uncertainty in the hydrogen EOS and astrophysical observations of the two planets. An improved experimental understanding of hydrogen at Mbar pressures and better determinations of the gravitational moments of both planets are necessary to put tight bounds on their internal structure.

Subject headings: planets and satellites: individual (Jupiter, Saturn) – equation of state

¹Dept. of Physics & Astronomy, Vanderbilt University, Nashville, TN, 37235-1807

1. Introduction

Dense hydrogen has been the subject of numerous theoretical and experimental studies over the last half century, in part because it has the simplest electronic structure of all the elements and because of its prevalence in the universe. This simplicity is only superficial however, as multiple experiments using static and dynamic compression to Mbar pressures have revealed increasingly complex properties and a rich phase diagram. For example, there are three known phases for the molecular solid (Mao and Hemley 1994), the molecular fluid becomes conducting at $P \gtrsim 1.4$ Mbar and $T \sim 4000$ K (Weir, Mitchell & Nellis 1996), the molecular nature of hydrogen persists to pressures above 3 Mbar (Loubeyre, Occelli & LeToullec 2002), and superfluid and superconducting phases have been suggested (Ashcroft 2003). Theoretical and experimental research on hydrogen is usually motivated by interest in warm dense matter problems in condensed matter physics, and applications to inertial confinement fusion research and to the interiors of giant planets. Indeed, Jupiter and Saturn are the largest reservoirs of fluid metallic hydrogen in the solar system and our understanding of these two planets depends rather critically on the properties of hydrogen, especially its equation of state (EOS).

Jupiter and Saturn are composed of about 50% to 70% hydrogen by mass. At pressures of $P \sim 1 - 3$ Mbar (corresponding to $\sim 80\%$ and $\sim 60\%$ of the planet's radius for Jupiter and Saturn, respectively), hydrogen goes from an insulating molecular fluid to an atomic metallic fluid. This transition has been the subject of much theoretical and experimental work but remains poorly understood. Recent shock compression experiments of deuterium to Mbar pressures disagree significantly (Collins et al. 1998; Knudson et al. 2004; Belov et al. 2002).

The internal structure of jovian planets is inferred indirectly from their global properties. Their rapid rotation results in a noticeable deformation and a non-spherical gravitational field that can be expressed as an expansion in Legendre polynomials:

$$V(r, \theta) = -\frac{GM}{r} \left[1 - \sum_{n=1}^{\infty} \left(\frac{R_{\text{eq}}}{r} \right)^n J_n P_n(\cos \theta) \right], \quad (1)$$

where G is the gravitational constant, M the mass of the planet, R_{eq} its equatorial radius, and the coefficients J_n are given by

$$J_n = -\frac{1}{MR_{\text{eq}}^n} \int_V r'^n P_n(\cos \theta) \rho(r', \theta) d^3 r' \quad (2)$$

and are known as the gravitational moments. The integral is performed over the volume of the planet. To a very high degree of accuracy, the planet is in hydrostatic equilibrium

and the symmetry between the northern and southern hemispheres implies that $J_n = 0$ for odd n . The first three non-vanishing moments, J_2 , J_4 , and J_6 have been measured during spacecraft flybys of both planets. Combined with the total mass, the radius, and the rotation period of the planet, these provide integral constraints on the density profile of the planet $\rho(r, \theta)$. These constraints cannot be inverted to obtain the density profile, however. Instead, a simple model is assumed for the structure and composition of the rotating planet which is then subjected to the condition of hydrostatic equilibrium, including the rotational potential perturbation. Model parameters are adjusted to fit the observed constraints. The EOS provides the $P(\rho)$ relation needed to close the system of equations. The structure thus inferred is sensitive to the choice of hydrogen EOS used in the models.

The total amount of heavy elements and their distribution inside these two planets bear directly on their formation process by accretion of both gaseous and solid material from the protoplanetary nebula. It is generally thought that Jupiter and Saturn formed according to the core accretion model. In the regions where they formed, refractory compounds (most significantly, water) had condensed and formed small solid bodies. Collisional processes between these planetesimals led to the build up of cores of $10 - 20 M_{\oplus}$ (Pollack et al. 1996) of heavy elements that subsequently accreted the surrounding gas on a dynamical time scale to build the large planets that we see today.² Formation by a disk instability in the gaseous protoplanetary disk, which does not require a seed core of heavy elements, has also been suggested as a formation mechanism (Boss 2000). Whether formation occurred through core accretion or disk instability (or perhaps another mechanism) depends very much on the internal structure and distribution of heavy elements that we see today in these planets.

Since the last determination of the gravitational moments of Jupiter and Saturn two decades ago (Campbell & Synnott 1985; Campbell & Anderson 1989), modeling of the interiors of Jupiter and Saturn has been driven primarily by the availability of improved equations of state for hydrogen. Recently, measurements of the reshock temperature (Holmes, Ross & Nellis 1995), the development of laser-induced shock compression (DaSilva et al. 1997) and pulsed-power shock compression (Knudson et al. 2001) have provided a wealth of new data and fueled intense theoretical debate on the physics of hydrogen at Mbar pressures and temperatures of $\sim 10^4$ K. For the first time, there are experimental data that allow us to constrain the EOS of hydrogen inside jovian planets at pressures of $\gtrsim 1$ Mbar, where the EOS remains most uncertain. Experimental results along the principal Hugoniot³ of

²The total masses are $317.83 M_{\oplus}$ and $95.147 M_{\oplus}$ for Jupiter and Saturn, respectively.

³A Hugoniot is a curve in (P, V, T) space that represents all the possible shocked states that can be achieved from a given initial state (P_0, V_0, T_0) .

deuterium do not agree (Collins et al. 1998; Knudson et al. 2001) in this pressure range. Laser compression data give a maximum compression of ~ 6 (DaSilva et al. 1997; Collins et al. 1998) while the pulsed-power compression experiments (Knudson et al. (2001)) and convergent spherical shock wave experiments (Belov et al. 2002; Boriskov et al. 2003) find a value of ~ 4 . Further study will reveal which experimental result is correct. However, it is generally agreed that the actual Hugoniot does not lie outside the range allowed by the current experiments. It is now possible to assign realistic error bars on the principal Hugoniot of deuterium, and hence on the EOS at pressures of a few Mbar. Until now, estimating the uncertainties on the EOS of hydrogen at these pressures had been little more than guess work.

In view of these new developments, a new study of the interiors of Jupiter and Saturn is warranted. In this paper, we examine how the uncertainty on the EOS of hydrogen maps unto uncertainties on the interior structure of Jupiter and Saturn. The resulting range of models provide firm bounds on the amount and distribution of heavy elements in these two planets. We first generated a number of EOS, supplemented with existing tabular EOS to represent subsets of (P, V, T) data along the principal and reshock Hugoniots of deuterium. Together, these EOS give Hugoniots that reproduce the extremes found in the data as well as intermediate behavior. The EOS are described in section 2. The computation of interior models of Jupiter and Saturn, described in section 3, includes many improvements over previous work. We present the new models and the effect of the hydrogen EOS on the cooling time scale of Jupiter in sections 4 and 5, respectively. The astrophysical implications are discussed in section 6.

2. Equations of State

2.1. Interior structures and relevant experimental data

The interiors of Jupiter and Saturn are believed to be mostly convective. The very high efficiency of convection inside jovian planets leads to a very small superadiabaticity so that the planets' interiors should be fully adiabatic for all practical purposes. This assumption may break down in several regions: (i) near the planets' cores, if conduction by degenerate electrons becomes efficient enough, or if a gradient of molecular weight is present; (ii) in a region at ~ 1 Mbar where helium would become less soluble in metallic hydrogen; (iii) at the molecular-metallic transition of hydrogen, if it is discontinuous; (iv) at ~ 1 kbar levels if alkali metals are not present (i.e. if their abundances is significantly less than solar); (v) in the “meteorological layer” ($P \sim 0.3 - 40$ bar), where the condensation of water affects the temperature gradients, chemical composition and horizontal homogeneity. None of these

possibilities can be dismissed at present but it can be advocated that none of them may cause a significant departure of the interior profile from adiabaticity (Guillot et al. 2003). In the absence of further information, adiabaticity of the interior profile is a perfectly valid working hypothesis.

The structure of the fluid envelopes of the giant planets is thus fixed by their specific entropy determined from observations of the surface. On the other hand, shock-compression experiments follow Hugoniots that are typically much hotter than the Jupiter and Saturn adiabats for the pressures of interest. For example, at 1 Mbar the temperature inside Jupiter is ~ 6000 K, while the principal Hugoniot reaches ~ 20000 K. The gas-gun reshock experiments overlap Jupiter’s adiabat up to 0.8 Mbar, however (Figs. 1 and 2).

Because of the limited overlap between Hugoniot data and the jovian planet adiabats, it is necessary to rely on model EOS anchored to the Hugoniot data to compute adiabats. This implies that two EOS models that predict nearly identical Hugoniots may produce different adiabats. For the purposes of this study, we computed interior models of Jupiter and Saturn with 7 different hydrogen EOS. These have been chosen as representative EOS that reproduce selected subsets of data and realistically bracket the actual EOS of hydrogen.

For simplicity, we consider only the following experiments:

- The (P, V) principal Hugoniot measured with the Z-machine at Sandia National Laboratory (Knudson et al. 2001, 2003, 2004) and two Hugoniot points achieved by convergent spherical shock wave compression (Belov et al. 2002; Boriskov et al. 2003). These data indicate a maximum compression of ~ 4 for deuterium along the Hugoniot.
- The (P, V) principal Hugoniot measured at the NOVA facility at Lawrence Livermore National Laboratory (DaSilva et al. 1997; Collins et al. 1998). These data indicate a maximum compression of ~ 6 for deuterium along the Hugoniot.
- The (P, T) data along the principal Hugoniot measured at the NOVA facility (Collins et al. 2001).
- The single and double shock gas gun T measurements (Holmes et al. 1995). The double shock temperatures may be systematically underestimated due to unquantified thermal conduction into the window upon shock reflection. We consider this data set as a lower limit on the reshock temperatures.
- The single and double shock gas gun (P, V) measurements (van Thiel et al. 1974; Nellis et al. 1983).

Together, these experiments characterize the principal and reshock Hugoniots of deuterium and the full range of current uncertainties quite well. Shock reverberation (Knudson et al. 2003) and laser reshock experiments to several Mbar (Mostovych et al. 2000; Boehly et al. 2004) have been shown to be generally consistent with (or to fall in between) EOS that we consider below, or similar EOS models.

2.2. Equations of State for Hydrogen

We have developed 4 different EOS based on the simple linear mixing model (hereafter, LM) devised by Ross (Holmes et al. 1995; Ross 1998, 1999) to reproduce the unexpectedly low gas-gun reshock temperature measurements (Holmes et al. 1995). The linear mixing model is based on a linear interpolation in composition between a molecular fluid and a metallic fluid:

$$F = (1 - x)F_{\text{mol}} + 2x(F_{\text{met}} + F_{\text{fit}}) - TS_{\text{mix}}(x), \quad (3)$$

where F is the total Helmholtz free energy per 2 atoms, F_{mol} and F_{met} are the free energies of the molecular and metallic fluids, respectively, x is the fraction of dissociated molecules, and $S_{\text{mix}}(x)$ is the ideal entropy of mixing. The molecular free energy is obtained from fluid perturbation theory with a soft sphere reference potential and an effective H₂-H₂ pair potential fitted to the gas gun (P, V) data (Ross, Ree & Young 1983). All four EOS presented here thus produce the same molecular Hugoniot. The One Component Plasma (OCP) forms the basis of the metallic fluid free energy, with a zero-temperature electron EOS including exchange and correlation (Holmes et al. 1995). An entropy term ($F_{\text{fit}} = \delta_e kT$, where k is the Boltzmann constant) is introduced in the metallic free energy and adjusted to fit the reshock temperature data ($\delta_e = -2.7$). This model was found to agree well with the subsequent NOVA Hugoniot (Collins et al. 1998; DaSilva et al. 1997) with the same value of δ_e . The LM model is particularly useful for the present study as it can be easily modified to fit various data sets.

We found that the original LM model (Ross 1998, 1999) predicts an anomalous adiabat for Jupiter. This can be seen in a sequence of adiabats with decreasing specific entropy (Fig. 3). The turnover of the adiabat around 1 Mbar has been reported before (Nellis, Ross & Holmes 1995) and is a direct consequence of fitting the reshock temperature measurements. At higher pressures, a cusp in the adiabat develops at low entropies. While this behavior is not strictly prohibited thermodynamically, it is very suspicious. It arises from the constant $\delta_e k$ shift in entropy of the metallic adiabats in the model. This causes a mismatch between the molecular and metallic adiabats that is significant when the entropy becomes small enough, as in Jupiter and Saturn. This means that while the original form of the LM

model reproduces the NOVA Hugoniot quite well, it is inadequate for EOS calculations at temperatures well below that of the principal Hugoniot.

We computed four LM EOS that produce better-behaved adiabats:

- **LM-A:** This EOS is identical to the original LM model (Ross 1998, 1999) except that the anomalous behavior of the adiabat has been corrected by replacing the fitting term $\delta_e kT$ by a temperature- and density-dependent contribution that is adjusted to fit Hugoniot data. The functional form is chosen for flexibility and to mimic the qualitative density dependence of electron screening:

$$\frac{F_{\text{fit}}}{kT} = \frac{-2.5}{1 + (0.8/V)^2} \left(\frac{5000}{T} \right)^{-0.1}, \quad (4)$$

where V is the specific volume in cm^3/mol , T the temperature in Kelvin and F_{fit} is the free energy per 2 atoms. The resulting EOS reproduces the NOVA (P,V,T) data and the reshock temperatures very well.

- **LM-B:** This EOS is identical to LM-A except that a steeper dependence on the specific volume V is used in F_{fit} :

$$\frac{F_{\text{fit}}}{kT} = \frac{-2.5}{1 + (1.5/V)^4} \left(\frac{5000}{T} \right)^{-0.1}. \quad (5)$$

The other parameters in Eq. (4) have been adjusted to fit the same data as with LM-A and their optimal values remain unchanged. In particular, the temperature dependance is tightly constrained by the NOVA (P, T) data (Collins et al. 2001). Higher powers of V in Eq. (5) cause a sharp minimum in the dissociation fraction x around $1.3 \text{ cm}^3/\text{mol}$ which is anomalous. The Hugoniots obtained for this form of F_{fit} are essentially identical to those of LM-A but the adiabat is stiffer and slightly hotter for $P \gtrsim 2 \text{ Mbar}$.

- **LM-SOCP:** In this model, the OCP model used by Ross for the metallic fluid is replaced by a more realistic screened OCP model (Chabrier 1990; Potekhin and Chabrier 2000) because electron screening is important in the regime found in the metallic envelopes of jovian planets. The electronic contributions to the free energy include finite temperature effects. In addition, we keep the entropy term of Ross and adjust it to approach the Sandia Hugoniot with $\delta_e = 0.5$. This (positive) value of δ_e is a compromise between fitting the low compressibility of the Sandia Hugoniot and the NOVA temperature measurements. The Sandia Hugoniot can be fit with $\delta_e = 2.0$ but the resulting principal Hugoniot temperatures are $> 2\sigma$ higher than the NOVA (P, T) data.

This model overestimates the reshock temperatures by $\sim 30\%$ and the maximum compression ratio of the Sandia and the spherical shock wave experiments by $\sim 15\%$.⁴ It is also a good representation of DFT-GGA simulations of deuterium (Lenosky et al. 2000) for $T \gtrsim 10^4$ K and $\rho \gtrsim 0.6$ g/cm³, *i.e.* outside of the molecular regime where these simulations miss the gas gun (P, V) data.

- **LM-H4:** In a variation on the LM EOS model, the need for a fitting term in the original LM model is removed by introducing D₄ chains as a new species (Ross and Yang 2001). This model considers a mixture of linear D₄ chains, D₂ molecules and a dissociated D⁺ + e⁻ fluid metal. Instead of the pair-wise linear mixing scheme used by Ross and Yang (2001), we apply a 3-component LM mixing scheme:

$$F = (1 - x - y)F_{D_4} + 2xF_{\text{mol}} + 4yF_{\text{met}} - TS_{\text{mix}}(x, y) \quad (6)$$

where F is the free energy per 4 atoms, x and y are the fractions of dissociated and ionized D₄ chains, respectively, $S_{\text{mix}}(x, y)$ is the ideal mixing entropy of the 3-component system, and F_{met} is the screened OCP free energy, as in LM-SOCP. This has a much larger effect than the choice of linear mixing scheme. The resulting EOS reproduces the NOVA (P, V, T) Hugoniot well but overestimates the reshock temperatures by $\sim 20\%$.

In all cases, the internal partition function of the molecules is calculated by an explicit sum over the known internal energy levels of H₂ or D₂ as appropriate. Similarly, proper isotope scaling was applied for the approximate vibrational and rotational properties of the chains (Ross and Yang 2001). These four EOS models were applied to deuterium to compare with shock compression experiments and to hydrogen to compute interior models of planets. These EOS are not intended to constitute practical EOS models for purposes other than this sensitivity study. They are rather simple representations of subsets of data that include enough physics to allow a reasonable calculation of adiabats.

Even though it predates all the shock compression experiments that we consider here, the **SESAME** deuterium EOS 5263 (Kerley 1972; SESAME library 1992) provides a fair representation of the Sandia Hugoniot and we adopt it here. For hydrogen, we adopt the SESAME EOS 5251 (SESAME library 1992), which is the deuterium EOS scaled in density. The SESAME 5251 table provides only $P(\rho, T)$ and $U(\rho, T)$. We computed the entropy by

⁴The convergent spherical shock wave experiment uses solid deuterium for its initial, unshocked state, with a density of $\rho_0 = 0.20$ g/cm³, compared to the liquid density of 0.17 g/cm³ used in the other experiments. This results in a slightly denser Hugoniot (Fig. 4) but the compression ratio (ρ/ρ_0) is very close to that of the Sandia experiment.

integrating the internal energy downward along isochores from a high- T isotherm obtained from the Saumon-Chabrier EOS (Saumon, Chabrier & Van Horn 1995). The calculated entropy does not recover the limit of the ideal H_2 gas, however. This is a consequence of the non-scalability of the molecular internal energy and entropy.

We found that in the molecular region ($P < 0.2$ Mbar), the SESAME deuterium Hugoniot is somewhat stiffer than indicated by the better measurements made after it was developed (Nellis et al. 1983). This is partly to blame for our inability to compute satisfactory models of Jupiter and Saturn with this EOS (see section 4). We have therefore patched the SESAME EOS in the molecular regime with an EOS that reproduces the low- P Hugoniot data such as any of the above linear mixing EOS. The patch is introduced by smoothly switching from one EOS to the other by applying the additive volume rule in the switching region, as if we were mixing two different substances. This preserves thermodynamic consistency. The transition is located between 0.1 kbar and 0.4 Mbar. We label this EOS **SESAME-p**. The resulting Hugoniots are nearly identical to SESAME Hugoniots, except at pressures below ~ 50 kbar. Because the SESAME entropy does not recover the ideal H_2 gas entropy at low density but the molecular EOS patch does, the SESAME-p adiabat is shifted to higher T and lower ρ at pressures above 10 kbar.

Finally, we computed models with the **SCVH-I** EOS (Saumon et al. 1995). Like the SESAME EOS, it predates all experiments except the (P, V) gas gun data which it reproduces by construction (like the four LM EOS above). It agrees better with the Sandia (P, V) Hugoniot for $P \lesssim 0.7$ Mbar and then shifts toward the NOVA Hugoniot at higher pressures across a small region where it is interpolated between the low-density and the high density EOS. The reshock temperatures are overestimated by $\sim 40\%$, but the agreement with the NOVA temperatures is good. This EOS has been used extensively in modeling the interiors of Jupiter and Saturn (Chabrier et al. 1992; Guillot et al. 1994, 1997; Guillot 1999; Gudkova and Zharkov 1999) and it serves as a basis for comparison.

Each EOS is compared with the various shock compression experiments in Figs. 4 and 5. This set of 7 EOS shows a range of behaviors that is representative of the possible range indicated by the experiments. The corresponding hydrogen adiabats for Jupiter are shown differentially with respect to the SCVH-I adiabat in Figs. 1 and 2. The Saturn adiabats are very similar. Interestingly, the variation among the adiabats in (P, ρ) (Fig. 1) is rather modest. By considering both the experimental error bars, the discrepancies between various experiments and a range of EOS models, we can estimate the uncertainty in the density along the Jupiter adiabat. The error bar on the adiabat density is vanishingly small at 1 bar (where the gas is ideal), and remains below 0.5% up to 1 kbar. It grows steadily from 2% at 30 kbar to 8% at 6 Mbar. The uncertainty decreases to about 3% at 100 Mbar because the

fluid is increasingly ionized and the EOS is more easily modeled. This small uncertainty on the (P, ρ) relation along the adiabat is large enough to affect the interior structure of the models. We find that the temperature along the adiabat (Fig. 2) is much more sensitive to the choice of EOS model. Variations are typically of $\sim 25\%$ above 3 Mbar and can be as large as 60%. This affects the thermal energy content of the planet and the time it takes to cool to its present state. The LM-A and LM-B adiabats are particularly cool at pressures above 1 Mbar.

2.3. Equations of State for Helium

Helium globally accounts for about 10% of the atoms in the jovian planets. Very little data and few EOS are available for helium in the regime of interest for jovian planets. There is only one set of four Hugoniot measurements published for helium (Nellis et al. 1984), reaching 0.6 Mbar on the reshock. Static compression experiments reach similar pressures at room temperature (Loubeyre et al. 1993). The EOS of helium in the 1–100 Mbar range is therefore unconstrained by experiments. In view of the recent developments on the EOS of hydrogen, we should assume that the EOS of helium at Mbar pressures and temperatures of several thousand degrees is much more uncertain than that of hydrogen, a situation that is fortunately mitigated by its relatively low abundance in jovian planets. We investigate the importance of this additional source of uncertainty on the structures of Jupiter and Saturn using two different EOS.

- **He-SCVH:** This tabular EOS (Saumon et al. 1995) is based on fluid perturbation theory for the atomic fluid, with an effective He-He pair potential adjusted to fit the Hugoniot data, and a screened OCP model for the fully ionized, dense plasma (Chabrier 1990). Between these two regimes (roughly from 0.6 to 60 Mbar), the EOS is smoothly interpolated. Thus, most of the mass of Jupiter and Saturn falls in the interpolated part of the He-SCVH EOS. This helium EOS has been used extensively in models of Jupiter and Saturn (Chabrier et al. 1992; Guillot et al. 1994, 1997; Guillot 1999; Gudkova and Zharkov 1999).
- **He-SESAME-p:** The SESAME EOS 5761 for helium (SESAME library 1992) predates the Hugoniot data (Nellis et al. 1984) but nevertheless reproduces them fairly well, although it is somewhat softer than the data indicates. To generate the entropy for the calculation of adiabats, we integrated the internal energy table along isochores as we did for the SESAME hydrogen EOS. There are some small anomalies in the internal energy in the regime of Saha ionization that result in low-density entropies

that deviate from the ideal gas limit for $T < T_{\text{ioniz}}$ by 4–5%. To remediate these limitations, we have patched the SESAME helium EOS for pressures below 10 kbar with the He-SCVH EOS following the same procedure as for the SESAME-p hydrogen EOS.

Figure 6 compares the two helium EOS along the (P, T) path defined by the *hydrogen* adiabat for Jupiter. The latter is a good approximation to the actual adiabat for a jovian mixture of hydrogen, helium, and heavy elements. The SESAME EOS becomes softer for $P \gtrsim 10$ kbar and then significantly stiffer above 1 Mbar. Not surprisingly, the difference between the two He EOS is larger than the most extreme differences found in the H EOS (Fig. 1).

3. The construction of interior models

The method used to compute interior models of Jupiter and Saturn has been presented elsewhere (Guillot et al. 1994; Guillot 1999) and will only be summarized here. Their interiors are assumed to consist of three mostly homogeneous regions:

1. A central dense core of mass M_{core} to be determined and of unknown composition;
2. An inner helium-rich envelope, assumed to coincide with the metallic hydrogen region;
3. An outer helium-poor envelope, whose helium abundance is constrained by spectroscopic and *in situ* measurements of the atmosphere.

The presence of a central core is generally needed to fit the planets' gravity fields. It is also qualitatively consistent with models in which the giant planets are formed by first accretion of a central seed of solids in the otherwise gaseous protosolar nebula (Pollack et al. 1996). The division of the hydrogen-helium envelopes into an inner and an outer part arises because the observed helium atmospheric abundances in Jupiter (von Zahn, Hunten & Lehmacher 1998) and Saturn (Conrath & Gautier 2000) are reduced compared to the protosolar value (Bahcall, Pinsonneault & Wasserburg 1995). It is speculated that hydrogen and helium undergo a phase separation for $T \lesssim 5000$ K and pressure of a few Mbar (Stevenson 1975). The formation of helium-rich droplets that sink deeper into the planet would explain the reduced atmospheric helium abundance. It would also provide an additional source of energy that is needed to understand Saturn's evolution, but could become a problem for Jupiter as it would tend to prolong its cooling beyond the age of the Solar System (Stevenson & Salpeter 1977; Fortney & Hubbard 2003; Guillot et al. 2003). In the absence of an

abundant species susceptible to separate from hydrogen (apart from helium), we assume that all heavy elements are homogeneously mixed in the envelope.

Given these simplifying assumptions, the only two parameters that we seek are the mass of the central core M_{core} and the mass of heavy elements mixed in the hydrogen-helium envelope, M_z . The value of these parameters are determined by an optimization technique aimed at finding models that match the observational values of the planets' equatorial radii R_{eq} and gravitational moments J_2 and J_4 within their error bars (Guillot et al. 1994; Guillot 1999). Due to large experimental uncertainties, J_6 does not further constrain the models.

The following uncertainties are taken into account:

1. The central core is assumed to be formed either from “rocks” (e.g. silicates and iron) or from “ices” (e.g. water, methane, ammonia);
2. The mass fraction of rocks in the envelope is varied between 0 and 4%;
3. The temperature at 1 bar, which determines the specific entropy of the adiabatic structure, is between 165 and 170 K for Jupiter and between 135 and 145 K for Saturn;
4. The ratio of helium to hydrogen abundance in the atmosphere is set to the in situ measurement for Jupiter (von Zahn et al. 1998) and the inferred spectroscopic measurement for Saturn (Conrath & Gautier 2000). The overall helium to hydrogen ratio in the entire planet is set equal to the protosolar value inferred from solar interior models (Bahcall et al. 1995). Both values are varied by $\pm 1\sigma$;
5. The location of the transition from the inner helium-rich to the outer helium-poor region is varied between 1 and 7 Mbar for Jupiter, and between 1 and 3 Mbar for Saturn;
6. Jupiter and Saturn are assumed to either rotate on concentric cylinders following observed zonal winds at the surface, or to rotate as solid bodies (Hubbard 1982).

Contrary to previous work, we do not allow for compositional discontinuities in the abundances of heavy elements in the envelope. We also assume that the temperature profile is adiabatic, as any radiative layer, if present at all, should be confined to a small region (Guillot et al. 2003). The hydrostatic structure is computed with the theory of rotating figures developed to the 4th order in the rotational perturbation.

We use the EOS for hydrogen and helium as described in Section 2. As an improvement over the previous models, we explicitly take the EOS of rocks and ices into account. We use

the SESAME EOS 7154 of water (SESAME library 1992) as a proxy for all ices (H_2O being by far the most abundant) and the SESAME EOS 7100 of dry sand (SESAME library 1992) for the rock-forming heavy elements. We account for the condensation of rocks/silicates in an approximate fashion by setting their abundance to zero for temperatures $T < 2500$ K. Water condenses around 300 K, but this is not included as it has a negligible effect on the interior structure and gravitational moments. In the absence of a suitable theory, the EOS of mixtures of H, He, water, and dry sand is obtained by applying the additive volume rule (see §4.1, however).

The 3-layer model is simplistic and the interiors of Jupiter and Saturn are undoubtedly more complex. Due to the scarcity of data and its current level of precision, more elaborate models are not justified at this point, however. We believe that the most significant sources of uncertainty have been taken into account in this study, which represents the most extensive sequence of interior models computed for Jupiter and Saturn so far.

4. New optimized interior models

4.1. Jupiter

For each EOS considered, a range of core masses (M_{core}) and masses of heavy elements in the envelope (M_z) is obtained after varying the other parameters and rejecting models that do not reproduce the gravitational moments.

Results obtained for Jupiter by only fitting R_{eq} and J_2 are shown in Fig. 7. What is particularly striking is that there is very little overlap between the solutions for the different EOS and that the result for the basic interior properties, M_{core} and M_z , greatly depends on the choice of EOS. Note for example that the LM-A and the LM-B EOS predict identical Hugoniots, but yield very different interiors. Quantitatively, this is due to the fact that the LM-B adiabat is $\sim 10\%$ less dense than the LM-A adiabat between 0.2 and 15 Mbar (Fig. 1).

The SESAME EOS combination of a low compressibility for $0.01 < P < 3$ Mbar and a high compressibility at larger pressures pushes the core mass downward. Surprisingly, even models with $M_{\text{core}} = 0$ do not fit Jupiter's R_{eq} and J_2 . This probably means that the SESAME EOS is too crude, but alternatively, that Jupiter's interior might be more complex than assumed here. A very small set of models with $M_{\text{core}} \sim 1 M_{\oplus}$ and $M_z \sim 33 M_{\oplus}$ were found with the SESAME-p EOS (which was softened in the low-pressure molecular region to be consistent with low-pressure experimental data).

Figure 8 shows the same results but including the constraint on J_4 . A noticeable con-

sequence is that LM-B EOS no longer satisfies the constraints. In fact, the values of J_4 found with this EOS are always more than 2σ away from the observed value (towards a higher absolute $|J_4|$). This EOS can apparently be ruled out. All other EOS show solution ensembles that barely differ from Fig. 7. In fact, models based on the SCVH-I EOS are the only ones that can be further constrained by the value of J_4 , as the upper-right part of the box in Fig. 7 corresponds to values of J_4 which lie 1 to 2σ away from the observed value. The absence of any further change for the other EOS shows that most of the constraints on Jupiter’s interior stem from the inferred radius and J_2 . The measured J_4 is useful, but it is not known with a sufficient accuracy yet to play an important role in the determination of M_{core} and M_z .

In order to estimate the robustness of the (M_{core}, M_z) ensemble of solutions for a given EOS, we considered models in which the density profile along the adiabat is arbitrarily modified by 2% according to:

$$\rho(P) = \rho_0(P) \left\{ 1 \pm 0.02 e^{-[\log_{10}(P/P_0)]^2} \right\}, \quad (7)$$

where ρ_0 is the unperturbed density and P_0 is varied from 3 to 100 Mbar. This provides an estimate of the remaining uncertainty on the adiabat computed from a given H EOS model and accounts for the approximate nature of the additive volume rule that we use to generate the EOS of the mixture of hydrogen, helium, rocks, and ices. Figure 9 shows that the resulting core masses and mass of heavy elements in the envelope globally lie relatively close to the solutions calculated without that additional uncertainty. In particular, the modification is not sufficient to salvage the LM-B EOS, whose resulting models still have J_4 values that are outside the 2σ observational error bars.

Quantitatively, we find that in Jupiter, $0 \leq M_{\text{core}} \lesssim 11 M_{\oplus}$ and $1 \lesssim M_z \lesssim 39 M_{\oplus}$. The total amount of heavy elements $M_{\text{core}} + M_z$ is 8 to $39 M_{\oplus}$. Compared to the abundance of heavy elements in the Sun, this corresponds to an enrichment by a factor of 1.5 to 6, which is consistent with the enrichment observed in Jupiter’s atmosphere. Since the full range of solutions is quite a bit larger than allowed for any given EOS, it implies that the uncertainty associated with the hydrogen EOS is more significant than all of the other uncertainties taken together. Furthermore, it is not yet possible to determine with any confidence the mass of the core of Jupiter or whether it has a core at all! Similarly, the total content of heavy elements is even less constrained. Only the LM-A EOS predicts a core mass as high as $11 M_{\oplus}$, which is marginally consistent with the core accretion formation model (which normally requires $10 - 20 M_{\oplus}$). All the others predict cores at most half as massive.

A comparison of Figs. 4, 5 and 8 shows that the hydrogen EOS that produce softer principal Hugoniots (i.e. reach higher maximum compression) give models with somewhat

larger M_{core} and smaller M_z . Further explorations with additional hydrogen EOS reveal that this trend is only apparent, however. Stiff EOS can lead to value of M_z nearly as small as those from the softest EOS. In other words, the EOS *model* fitted to the experimental data used to compute the adiabat is just as important as the experimental data themselves in determining the internal structure of Jupiter. This points to the importance of measuring the EOS of hydrogen closer to the Jupiter isentrope.

4.2. Jupiter: Uncertainties related to the He EOS

In order to estimate uncertainties due to the helium EOS, we calculated Jupiter models with the same hydrogen EOS as described previously, but using the He-SESAME-p EOS instead of the He-SCVH EOS (see section II.C). The two EOS differ only slightly, but the systematic deviation in both entropy and density lead to a $\sim 2\%$ reduction in density along the adiabat of the mixture for $P \gtrsim 3$ Mbar.

The consequences are shown in Fig. 10. With the new He-SESAME-p, the core mass is found to be systematically larger. This is explained by the fact that the 2% reduction in the density of the mixture needs to be compensated by an additional $\sim 2\% \times 318 M_{\oplus} \sim 6 M_{\oplus}$ mass of heavy elements, to be distributed between M_{core} and M_z . Another consequence is a displacement of the resulting value of J_4 , for any model fitting R_{eq} and J_2 (see Fig.5 of Guillot (Guillot 1999)). The new values are such that $|J_4|$ is higher by about $0.5 - 1\sigma$. This implies that solutions with the LM-B hydrogen EOS are even further from the observations than before. It has little consequences for other EOS, except for the SCVH-I solutions which now always have a J_4 value that is at least 1σ away from the measurements. Although the solutions set by R_{eq} and J_2 have moved to higher values of M_{core} and M_z , the J_4 constraint reduces the size of the effect.

4.3. Saturn

The mass of Saturn is slightly below $1/3$ that of Jupiter and as a consequence, only 67% of its mass lies at $P > 1$ Mbar, compared to 91% for Jupiter. Saturn is therefore less sensitive to the larger EOS uncertainties than Jupiter. Saturn's response to rotation is also qualitatively different, as can be seen from its linear response coefficient: $\Lambda_2 \approx J_2/q$ where $q = \omega^2 R_{\text{eq}}^3/GM$ is the ratio of the centrifugal to the gravitational potentials. The value of Λ_2 is 0.108 for Saturn compared to 0.166 for Jupiter, implying that Saturn's interior is more concentrated, i.e. it is expected to have a proportionally larger core than Jupiter (Hubbard

1989). Finally, the error bars on the gravitational moments J_2 and J_4 of Saturn are much larger than for Jupiter. We anticipate that the results will be qualitatively different.

The solutions for Saturn are summarized in Fig. 11. We present only the case where the 2% perturbation on the EOS (Eq. 7) has been included as this has only a slight effect on Saturn models. We find that there is much more overlap between the solutions for the different EOS than is the case for Jupiter and that we can usefully constrain the core mass and the mass of heavy elements in the envelope to $9 \lesssim M_{\text{core}} \lesssim 22 M_{\oplus}$ and $1 \lesssim M_z \lesssim 8 M_{\oplus}$ for a total mass of heavy elements between 13 and $28 M_{\oplus}$. The EOS is an important source of uncertainty in modeling Saturn’s interior but it is not as dominant as in Jupiter. We also find that the LM-B EOS and the original SESAME EOS (not shown) give acceptable models of Saturn. The amount of heavy elements in the envelope is rather modest but the total amount of heavy elements in Saturn represents a 6- to 14-fold enrichment compared to the solar value. Saturn may contain more heavy elements than Jupiter. The choice of EOS has no discernible effect on M_{core} , however, and the uncertainty on the helium EOS barely affects the ensemble of solutions for Saturn. The distribution and the amount of heavy elements in Saturn is in very good agreement with the core accretion formation model.

5. Evolution of Jupiter

While the (P, ρ) relation along the adiabat determines the internal structure of the planet, the (P, T) relation influences its cooling age by setting its internal heat content. The cooling rate itself is determined by the rate at which heat can escape at the surface, which is controlled by the atmosphere of the planet, treated as a surface boundary condition in the cooling calculation. In section 4, we showed how rather modest variations in density along the adiabat (Fig. 1) are responsible for astrophysically significant changes in internal structure. The variations in adiabat temperatures between the EOS can be as large as 60%. The largest variations occur at pressures above 1 Mbar and involve most of the mass of Jupiter and Saturn.

In order to test the effect of the EOS on the evolution of the giant planets, we have computed homogeneous, adiabatic evolution calculations (i.e. without considering the possibility of a He/H phase separation) for Jupiter following the method described in Guillot et al. (1995). Although the resulting models only reproduce approximatively the present planetary structures (we only try to match the mean radius and intrinsic luminosity), it is a helpful indication of how the hydrogen EOS also affects the cooling of the giant planets. We do not present calculations for Saturn since its evolution is likely affected by the slow gravitational energy release from helium-rich droplets sinking toward the center due to H/He

demixing (Fortney & Hubbard 2003).

For each choice of EOS, initial conditions are determined by the structural parameters fitted to the observational constraints. The model is started at an arbitrary large value of the specific entropy, resulting in an initial radius $R \approx 1.15 - 1.5 R_{\text{Jup}}$. Because the planet initially cools very rapidly, the initial value of the entropy is not important as long as it is large enough (the corresponding uncertainty between the different models is ~ 50 Myr). The variation in internal heat content with the choice of EOS implies that Jupiter will cool to its present luminosity (and contract to its present radius) in more or less time. This cooling age is to be compared to the age of the Solar System of 4.56 Gyr.

Naturally, models computed with EOS that give cooler adiabats (such as LM-A and LM-B, see Fig. 2) have a lower internal heat content and will cool to the present luminosity in a shorter time, everything else being equal. The effect is quite significant, as can be seen in Fig. 12. We find that the cooling ages for each EOS are 5.4 Gyr (SESAME-p), 4.8 Gyr (LM-SOCP), 4.7 Gyr (SCVH-I), 4.0 Gyr (LM-H4), and 3.1 Gyr (LM-A). The absolute ages quoted here are only representative since they depend on a presently inaccurate surface boundary condition and do not include the possibility of a modest degree of phase separation in Jupiter which would lengthen the cooling time of all models (Fortney & Hubbard 2003). The relative ages are much less sensitive to these limitations.

Nevertheless, the cooling age obtained with the LM-A EOS is so short that it is unlikely that it could be reconciled with the age of the solar system with a more elaborate cooling calculation. Adiabats that are very cool above 1 Mbar are characteristic of the EOS that fit the reshock temperature data (LM-A, LM-B, and the even more extreme case of the original LM model of Ross shown in Fig. 3). On the other hand, it appears that the SESAME-p EOS leads to a cooling that is too slow to be consistent with the age of the Solar System. For the other EOS (LM-H4, SCVH-I and LM-SOCP), it can be advocated on one hand that energy release due to a H/He phase separation may lengthen the cooling (Fortney & Hubbard 2003), or on the other hand an efficient erosion of the central core may shorten it sufficiently to account for the observed discrepancy (Guillot et al. 2003).

6. Astrophysical implications and concluding remarks

We have computed a new generation of interior models for Jupiter and Saturn, with an emphasis on improving the treatment of the EOS of hydrogen and of elements heavier than H and He. In particular, we have used 7 different EOS of hydrogen that were chosen to reproduce the range of possibilities indicated by first and second shock Hugoniot data.

This allows, for the first time, a determination of the effects of the present uncertainty on the EOS of hydrogen on the interior structure of jovian planets. The parameters of interest, which characterize the total mass of heavy elements and their radial distribution in both Jupiter and Saturn are now constrained reliably by this study.

It is interesting to compare the results to previous models (Guillot et al. 1997; Guillot 1999) for which a third parameter was added to the optimization: a discontinuity in the abundance of heavy elements across the helium-poor/helium region (located at the transition between molecular and metallic hydrogen in the 3-layer model). Our results for Jupiter are very similar, in particular concerning the low central core mass and highly uncertain total mass of heavy elements. Differences arise in the case of Saturn, for which some models (Guillot 1999) were found to fit the planet’s gravitational field with no central dense core. However, these previous models consisted in solutions with a high abundance discontinuity at the molecular/metallic transition (a large abundance of heavy elements in the helium-rich region mimicking the effect of a central dense core). We can thus be relatively confident that even with a simple three-layer model with two free parameters (M_{core} and M_z) one can constrain the global structures of Jupiter and Saturn. On the other hand, we should keep in mind that the real structures of these two planets maybe more complex so that the actual interpretation of these parameters is not precisely defined (e.g. the central core could be either diluted or present as a well-defined structure).

Quantitatively, we confirm that both Jupiter and Saturn are enriched in heavy elements compared to the Sun, by factors of 1.5 – 6 and 6 – 14, respectively. Maximum compression ratios of ~ 4 along the principal Hugoniot are supported by three independent experiments (Knudson et al. 2001; Belov et al. 2002; Boriskov et al. 2003; Knudson et al. 2003, 2004), and by most ab initio EOS simulations (Lenosky, Kress & Collins 1997; Militzer & Ceperley 2000; Galli et al. 2000; Desjarlais 2003). This type of Hugoniot response is represented by the LM-SOCP and the SESAME-p EOS. Interestingly, both EOS lead to very small core masses ($M_{\text{core}} \lesssim 3 M_{\oplus}$) in Jupiter, and a substantial amount of heavy elements in the envelope. The same EOS predict a more massive core in Saturn ($10 - 20 M_{\oplus}$). Changing the He-SCVH helium EOS for the He-SESAME-p EOS has a modest effect on the structure of Jupiter and increases the total amount of heavy elements by a few Earth masses, split more or less evenly between the core and the envelope. This does not change the qualitative picture that emerges, however.

Taken at face value, these results imply that Jupiter formed by disk instability in the protoplanetary disk while Saturn formed by core accretion. It is rather unlikely that the two planets formed by such different mechanisms, however. We speculate that the only way to reconcile the formation processes of Jupiter and Saturn is that both of them formed by

core accretion and that for Jupiter, the subsequent accretion of the gaseous H/He envelope resulted in partial or complete mixing of the core with the gas, increasing M_z at the expense of M_{core} . The larger accretion rate in the proto-Jupiter may have caused larger mixing than in the proto-Saturn (Guillot et al. 2003).

On the other hand, Jupiter models computed with the LM-A EOS have core masses that are (barely) consistent with the mass required for formation with core accretion formation ($\sim 10 M_{\oplus}$). In this case, mixing of the core of proto-Jupiter with the accreting envelope would not be required and both planets would form by the same process. The LM-A EOS was constructed to fit the NOVA (P, V, T) Hugoniot as well as the gas gun reshock temperatures. It represents the softest and coolest EOS allowed by the experiments. The reshock temperatures measurements may be too low, however, and a reevaluation of these measurements may well rule out the LM-A EOS.

This study has been conducted with the point of view of learning about the interiors of Jupiter and Saturn from our current knowledge of the EOS of hydrogen and the associated uncertainties. The opposite approach can also be considered: Can astrophysical knowledge contribute to the debate on the high-pressure EOS of hydrogen? Because much astrophysical knowledge is not amenable to direct observation or experimentation, our knowledge of processes that are hidden from view or that are no longer taking place is very sketchy. It is usually difficult to draw strong conclusions about the underlying microphysics when only the global properties of a complex, natural object are known. The ability of a given EOS to give acceptable models depends somewhat on the assumptions for the model structure. In general, more elaborate models (with more parameters) can accommodate a wider range of EOS. Nevertheless, we venture to comment on interesting patterns that emerge in the more extreme cases that we have encountered in this study.

We could not obtain satisfactory models of Jupiter with the original SESAME EOS because it is relatively stiff between 0.1 and 3 Mbar, and relatively soft at higher pressures along Jupiter's adiabat. Both of these effects combine to decrease the core mass (Guillot 1999) but even with $M_{\text{core}} = 0$ models that fit the gravitational moments could not be obtained with this EOS. It is only after it was patched at low pressures and that a 2% uncertainty in the EOS was introduced that acceptable models could be found (SESAME-p EOS). Similarly, we could not obtain satisfactory models of Jupiter with the LM-B EOS because it is too stiff along the adiabat above 5 Mbar. Taken together, these constrain the (P, ρ) relation along the adiabat a little more than the experimental results alone (see Fig. 1). We find that most EOS predict relatively small core masses for Jupiter. While it may be possible to accommodate such a situation astrophysically, it would require a substantial revision of the generally accepted formation process of the planet. Cooling calculations

provide additional information. We find that EOS that fit the gas gun reshock temperatures (e.g. LM-A) give cooling times that are uncomfortably short for Jupiter, suggesting that those temperatures are systematically too low. Models of Saturn do not provide any useful information on the EOS of hydrogen.

Further progress in determining the interior structures of Jupiter and Saturn can be accomplished with a two-pronged approach. Proposed space missions to Jupiter would lead to a tenfold reduction of the uncertainty on its gravitational moments, greatly reducing the range of acceptable models (*i.e.* smaller boxes in Fig. 9). Such improved measurements would most likely lead to rather distinct solutions for different choices of hydrogen EOS. The Cassini spacecraft will enter Saturn orbit in July 2004 for a 4-year mission and could reduce the error bars on the gravitational moments significantly (in the context of an extended mission with accurate Saturn gravity measurements). This would greatly reduce the range of acceptable models (Fig. 11).

Improved astrophysical data will not be sufficient, however. It is as important to reduce the uncertainties surrounding the EOS of hydrogen in the 1 to 30 Mbar range. This can be achieved indirectly by reducing the experimental uncertainty along the principal Hugoniot, or by directly reproducing the conditions found inside giant planets with reshock and reverberation experiments (Knudson et al. 2003; Boehler et al. 2004). From the perspective of planetary science, two additional EOS problems deserve much attention. The EOS of helium and especially that of hydrogen/helium mixtures, with the possibility of a demixing phase transition, need to be investigated both experimentally and theoretically. The phase diagram of H/He mixtures is well-constrained by the astrophysics of Jupiter and Saturn, making this an especially interesting problem to study with the most advanced ab initio methods available.

This work was supported in part by NASA Planetary Geology & Geophysics grant NAG5-8906, by the United States Department of Energy under contract W-7405-ENG-36, and by the *Programme National de Planétologie* (France). We thank Bill Hubbard for sharing results and codes on rotating polytropic models, and Julie Castillo for thorough discussions on expected gravity measurements with Cassini.

REFERENCES

Ashcroft, N. W. 2003, *J. Phys. A: Math. Gen.*, 36, 6137

Bahcall, J. N., Pinsonneault, M. H. & Wasserburg, G. J. 1995, *Rev. Mod. Phys.*, 67, 781

Belov, S. I. et al., 2002, *JETP Lett.*, 76, 433

Boehly, T. R., Hicks, D. G., Celliers, P. M., Collins, T. J. B., Eggert, J. H., Moon, S. J., Vianello, E., Meyerhofer, D. D. & Collins, G. W. 2004, submitted to *Phys. Rev. Lett.*

Boriskov, G. V., Bykov, A. I., Il'Kaev, R. I., Selemir, V. D., Simakov, G. V., Trunin, R. F., Urlin, V. D., Fortov, V. E. & Shuikin, A. N. 2003, *Doklady Physics*, 48, 553

Boss, A. P. 2000, *ApJ*, 536, L101

Campbell, J. K. & Synnott, S. P. 1989, *AJ*, 90, 364

Campbell, J. K. & Anderson, J. D. 1989, *AJ* 97, 1485

Chabrier, G. 1990, *J. de Phys.*, 51, 1607

Chabrier, G., Saumon, D., Hubbard, W. B. & Lunine, J. I. 1992, *ApJ*, 391, 817

Collins, G. W. et al., 1998, *Science*, 281, 1178

Collins, G. W. et al., 2001, *Phys. Rev. Lett.*, 87, 165504

Conrath, B. J. & Gautier, D. 2000, *Icarus*, 144, 124

DaSilva, L. B. et al., 1997, *Phys. Rev. Lett.*, 78, 483

Desjarlais, M. P. 2003, *Phys. Rev. B*, 68, 64204

Fortney, J. J. & Hubbard, W. B. 2003, *Icarus*, 164, 228

Galli, G., Hood, R. Q., Hazi, A. U., & Gygi, F. 2000, *Phys. Rev. B*, 61, 909

Gudkova, T. V. & Zharkov, V. N. 1999, *Plan. Space Sci.*, 47, 1201

Guillot, T., Chabrier, G., Gautier, D. & Morel, P. 1995, *ApJ*, 450, 463

Guillot, T. 1999, *Plan. Space Sci.* 47, 1183

Guillot, T., Chabrier, G., Morel, P. & Gautier, D. 1994, *Icarus*, 112, 354

Guillot, T., Gautier, D., & Hubbard, W. B. 1997, *Icarus*, 130, 534

Guillot, T., Stevenson, D. J., Hubbard, W. H. & Saumon, D., 2003, in Jupiter, F. Bagenal, ed., (Cambridge Univ. Press: Cambridge), in press.

Holmes, N. C., Ross, M., & Nellis, W. J. 1995, Phys. Rev. B, 52, 15835

Hubbard, W. B. 1982, Icarus, 52, 509

Hubbard, W. B. 1989, in Origin and Evolution of Planetary and Satellite Atmospheres, S.K. Atreya et al. Eds., (Univ. Arizona: Tucson), 539

Kerley, G. I. 1972, Los Alamos Scientific Laboratory, Technical Report LA-4776, 1

Knudson, M. D., Hanson, D. L., Bailey, J. E., Hall, C. A. & Asay, J. R. 2001, Phys. Rev. Lett., 87, 225501

Knudson, M. D., Hanson, D. L., Bailey, J. E., Hall, C. A. & Asay, J. R. 2003, Phys. Rev. Lett., 90, 035505

Knudson, M. D. Hanson, D. L., Bailey, J. E., Hall, C. A., Asay, J. R. & Deeney, C. 2004 submitted to Phys. Rev. B

Lenosky, T. J., Bickham, S. R., Kress, J. D., & Collins, L. A. 2000, Phys. Rev. B, 61, 1

Lenosky, T. J., Kress, J. D. & Collins, L. A. 1997, Phys. Rev. B, 56, 5164

Loubeyre, P., LeToullec, R., Pinceaux, J. P., Mao, H.-k., Hu, J. & Hemley, R. J. 1993, Phys. Rev. Lett., 71, 2272

Loubeyre, P., Occelli, F. & LeToullec, R. 2002, Nature, 416, 613

Mao H.-k. & Hemley, R. J. 1994, Rev. Mod. Phys., 66, 671

Militzer B. & Ceperley, D. M. 2000, Phys. Rev. Lett., 85, 1890

Mostovych, A. N., Chan, Y., Lehecha, T., Smith, A. & Sethian J. D., 2000, Phys. Rev. Lett., 85, 3870

Nellis, W. J., Holmes, N. C., Mitchell, A. C., Trainor, R. J., Governo, G. K. Ross, M. & Young, D. A. 1984, Phys. Rev. Lett., 53, 1

Nellis, W. J., Mitchell, A. C., van Thiel, M., Devine, G. J. & Trainor, R. J. 1983, J. Chem. Phys., 79, 1480

Nellis, W. J., Ross, M., & Holmes, N. C. 1995, Science, 269, 1249

Pollack, J. B., Hubickyj, O., Bodenheimer, P., Lissauer, J. J., Podolak, M. & Greenzweig, Y. 1996, *Icarus*, 124, 62

Potekhin, A. Y. & Chabrier, G. 2000, *Phys. Rev. E*, 62, 8554

Ross, M. 1998, *Phys. Rev. B*, 58, 669

Ross, M. 1999, *Phys. Rev. B*, 60, 6923

Ross, M., Ree, F. H. & Young, D. A. 1983, *J. Chem. Phys.* 79, 1487

Ross, M. & Yang, L. H. 2001, *Phys. Rev. B*, 64, 134210

Saumon, D., Chabrier, G. & Van Horn, H. M. 1995, *ApJS*, 99, 713

Stevenson, D. J. 1975, *Phys. Rev. B*, 12, 3999

Stevenson, D. J. & Salpeter, E. E. 1977, *ApJS*, 35 239

SESAME: The Los Alamos National Laboratory Equation of State Database 1992, LANL Report No. LA-UR-92-3407, S. P. Lyon & J. D. Johnson (eds.)

van Thiel, M., Hord, L. B., Gust, W. H., Mitchell, A. C., D'Addario, M., Boutwell, K., Wilbarger, E. & Barret, B. 1974, *Phys. Earth. Plan. Inter.*, 9, 57

von Zahn, U., Hunten, D. M. & Lehmacher, G. 1998, *J. Geophys. Res.*, 103, 22815

Weir, S. T., Mitchell, A. C. & Nellis, W. J. 1996, *Phys. Rev. Lett.*, 76, 1860

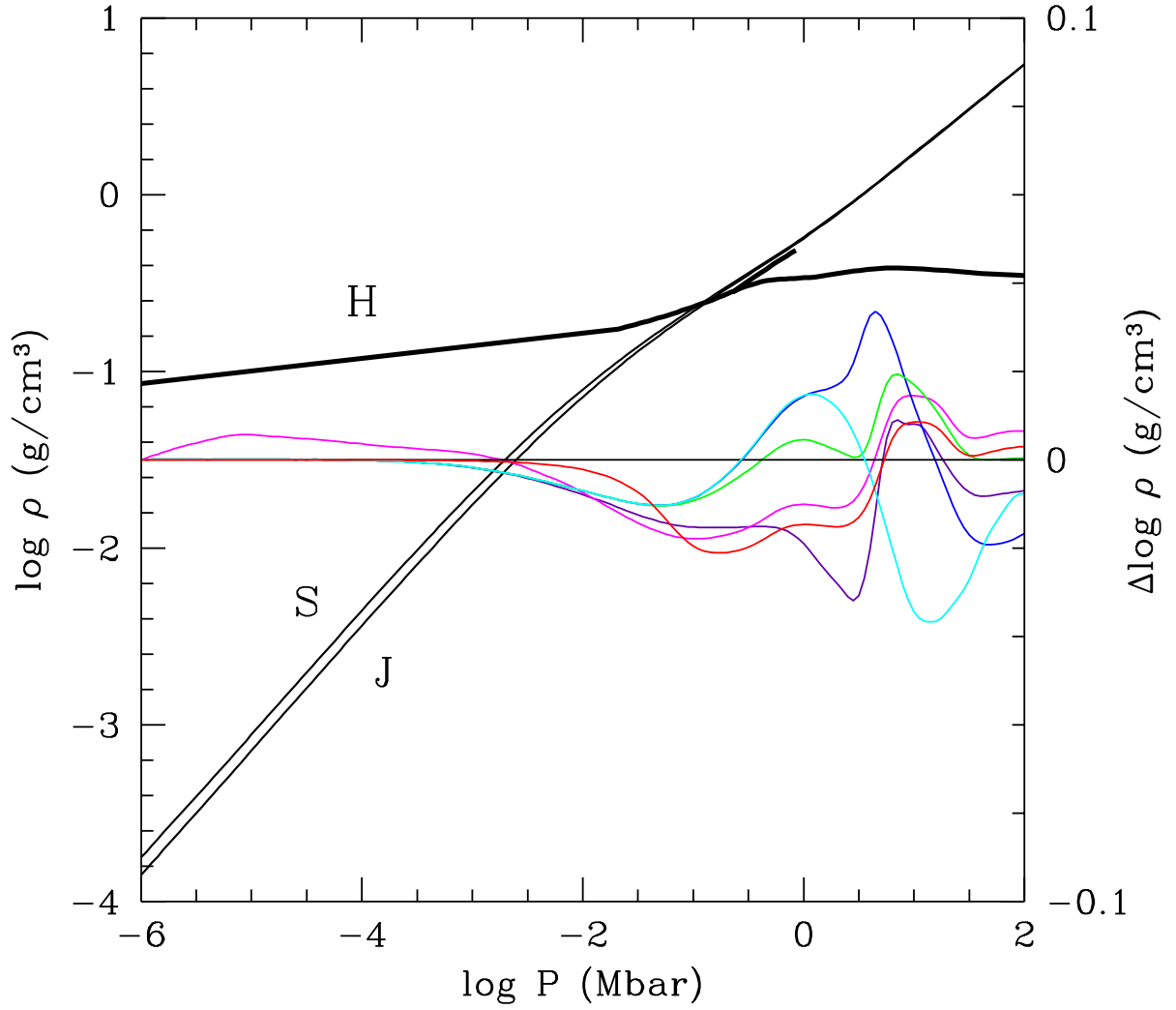


Fig. 1.— Adiabats for hydrogen in P – ρ . The curves labeled ‘S’ and ‘J’ show the SCVH-I EOS adiabats of Saturn and Jupiter, determined by $T = 136$ K and 170.4 K at $P = 1$ bar, respectively. The first and second-shock Hugoniots (SESAME EOS) are shown by the heavy solid line labeled ‘H’. The other curves and the scale on the right show *differences* in density between Jupiter adiabats computed with various EOS (see section 2.A), relative to the SCVH-I: SESAME (short dashes, magenta), SESAME-p (short dash - long dash, red), LM-A (long dashes, blue), LM-B (long dash - dot, cyan), LM-SOCP (dotted, purple), and LM-H4 (short dash - dot, green). The central pressure of Jupiter is about 70 Mbar and that of Saturn is about 40 Mbar. [See the electronic edition of the Journal for a color version of this figure.]

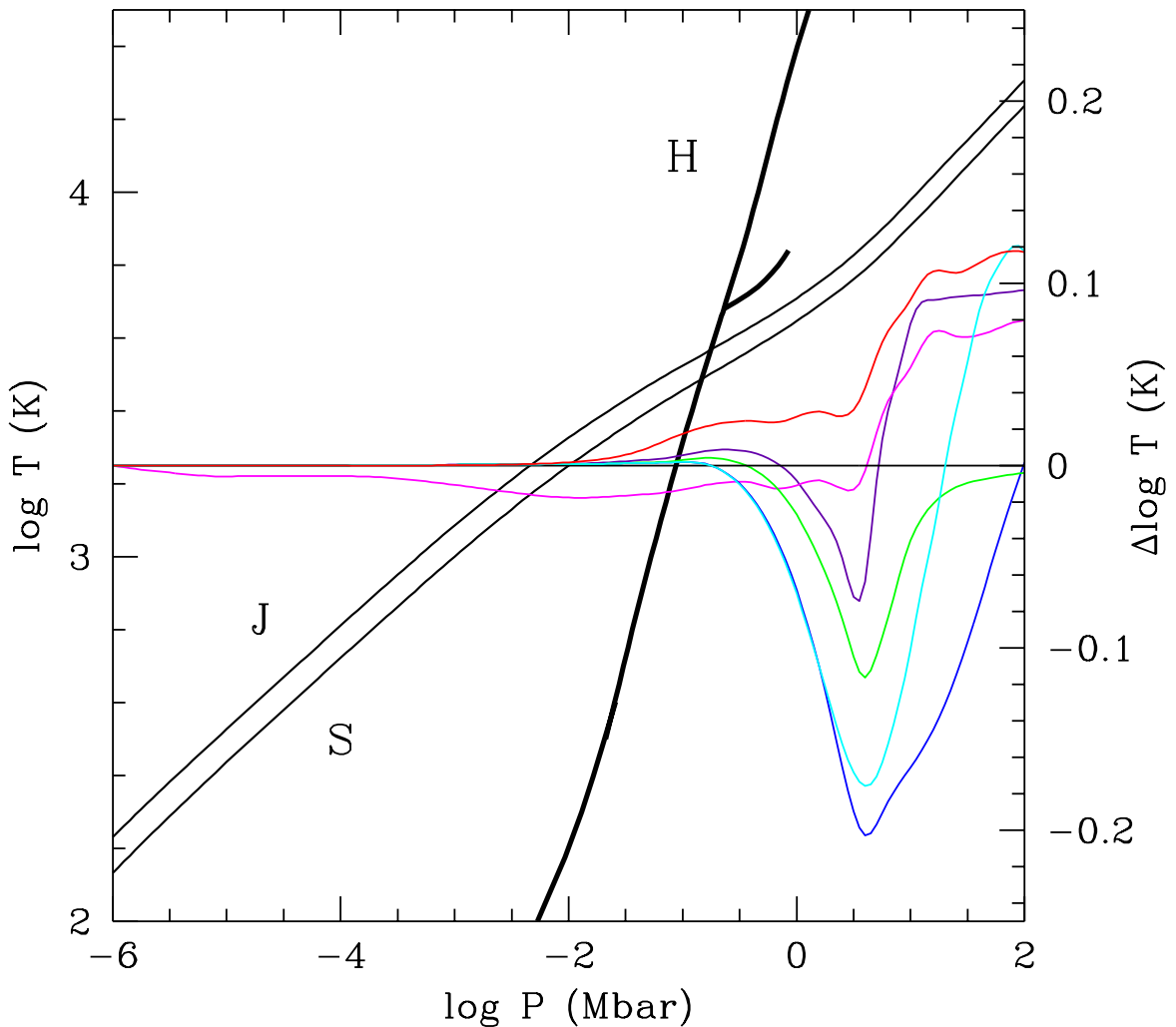


Fig. 2.— Adiabats for hydrogen in P – T . See the caption of Fig. 1 for details. [See the electronic edition of the Journal for a color version of this figure.]

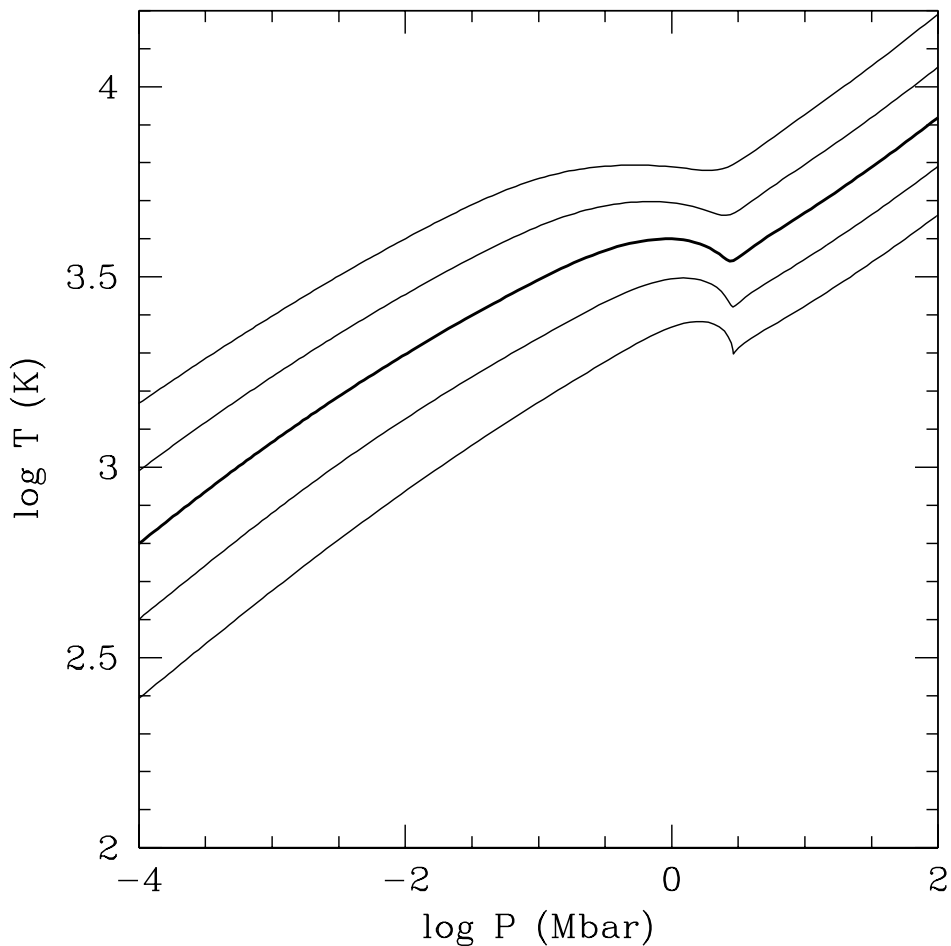


Fig. 3.— Adiabats for hydrogen computed with the linear mixing model of Ross (1998) for different specific entropies. The entropy decreases from top to bottom. Jupiter's adiabat is shown by the heavy solid line.

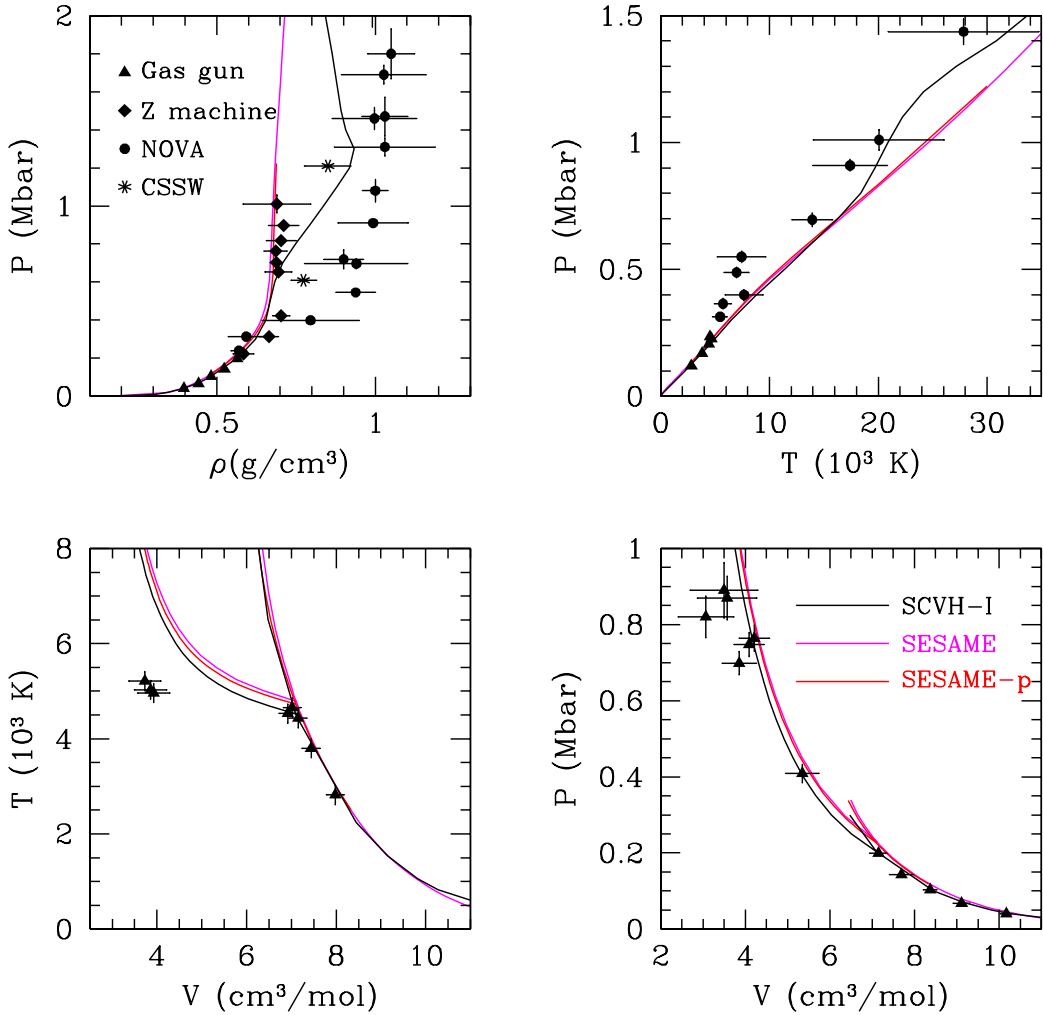


Fig. 4.— First and reshock Hugoniots of deuterium compared with experimental data. The Hugoniots are computed from the following EOS: SCVH-I, SESAME, and SESAME-p. Both versions of the SESAME EOS give very nearly identical Hugoniots. The experimental data includes gas gun data (van Thiel et al. 1974; Nellis et al. 1983; Holmes et al. 1995), the NOVA data (DaSilva et al. 1997; Collins et al. 1998, 2001), Z-machine measurements (Knudson et al. 2004) and one point from a convergent spherical shock wave compression experiment (Belov et al. 2002; Boriskov et al. 2003). [See the electronic edition of the Journal for a color version of this figure.]

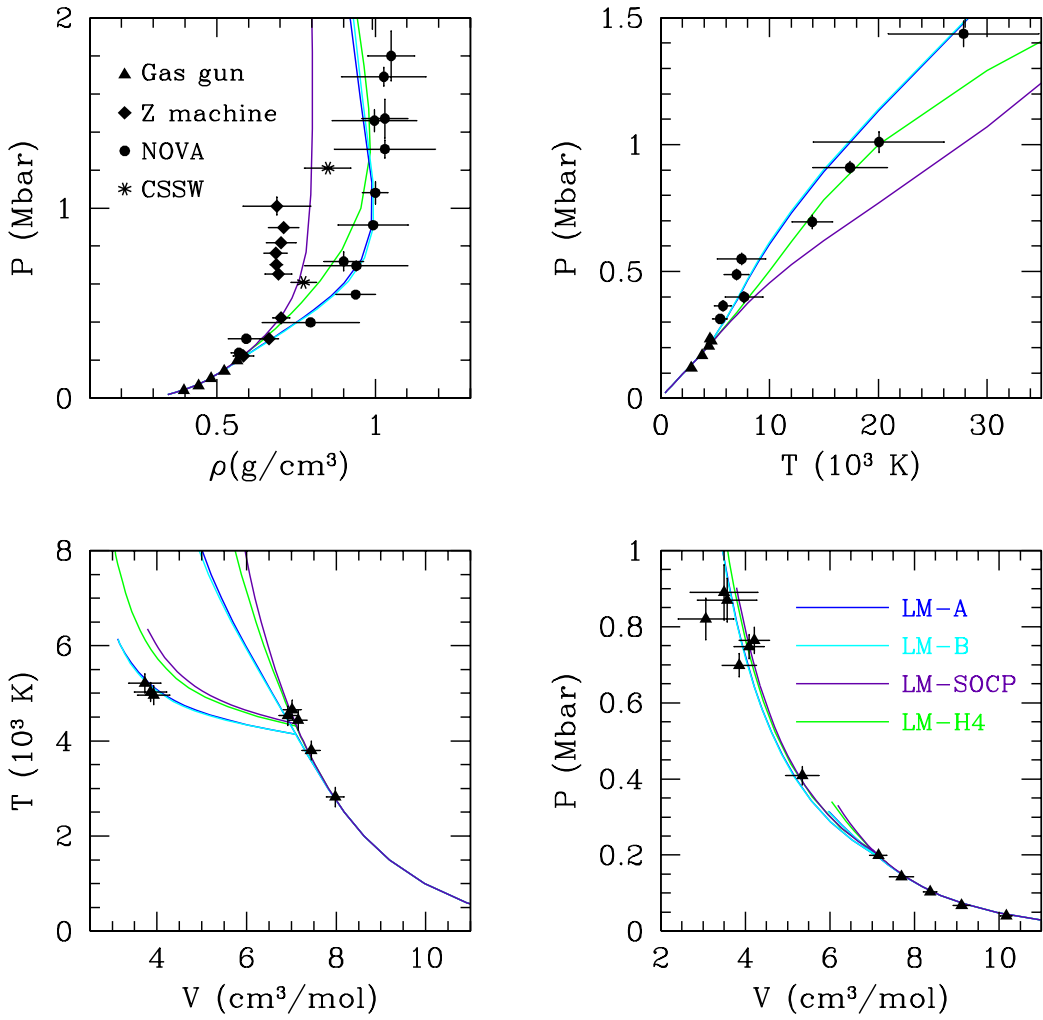


Fig. 5.— Same as Fig. 4 but for the following EOS: LM-A, LM-B, LM-SOCP, and LM-H4. The LM-A and LM-B Hugoniots are very nearly identical. [See the electronic edition of the Journal for a color version of this figure.]

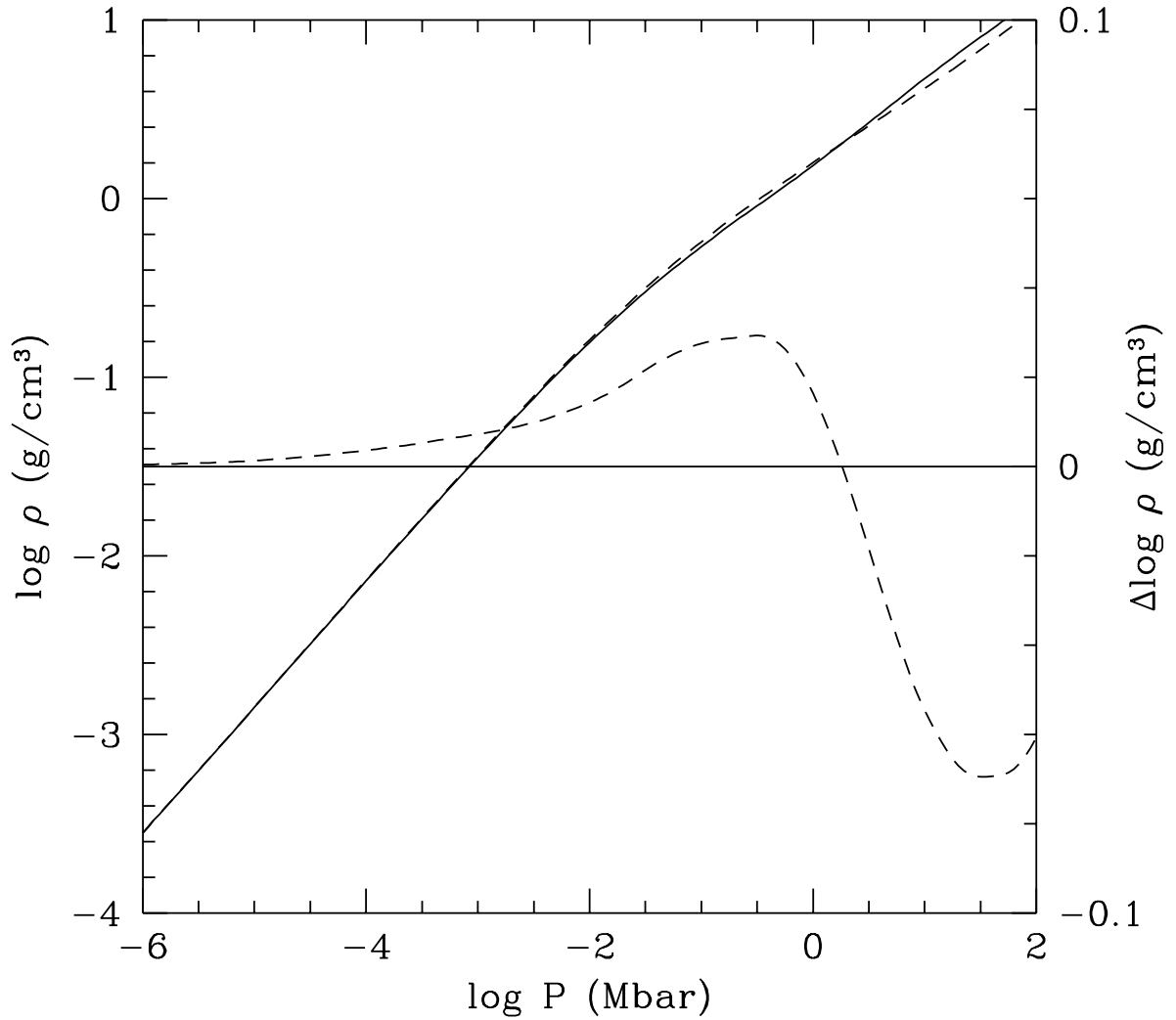


Fig. 6.— Density of helium along the (P, T) adiabat of Jupiter for hydrogen (diagonal curves). Two EOS are shown: He-SCVH (solid) and He-SESAME-p (dashed). The difference between the two adiabats is shown on the scale at right.

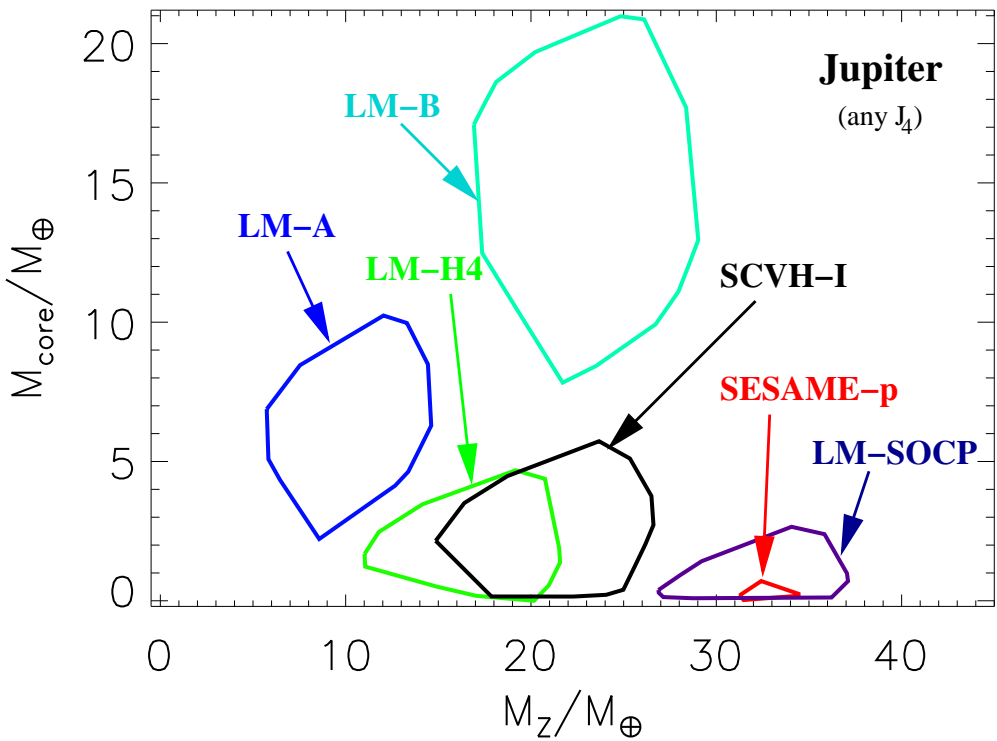


Fig. 7.— Jupiter’s core mass M_{core} and mass of heavy elements mixed in the H/He envelope M_z in Earth masses (M_{\oplus}). The total mass of Jupiter is $317.83 M_{\oplus}$. Each box represents the range of models that match Jupiter’s equatorial radius and gravitational moment J_2 for a given choice of hydrogen EOS, including all the parameter variations described in the text. The models do not necessarily have the correct value of J_4 . [See the electronic edition of the Journal for a color version of this figure.]

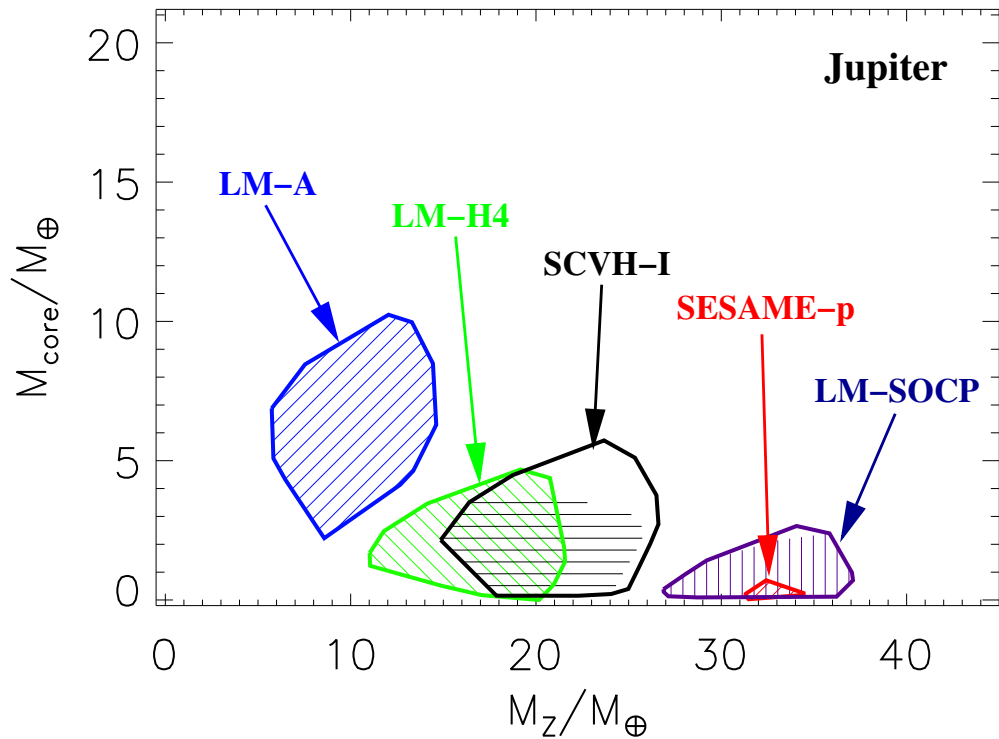


Fig. 8.— Same as Fig. 7 but each box represents the range of models that match Jupiter's R_{eq} , J_2 and J_4 within 2σ of the observed value. The hashed regions corresponds to models that match J_4 within 1σ of the observations. [See the electronic edition of the Journal for a color version of this figure.]

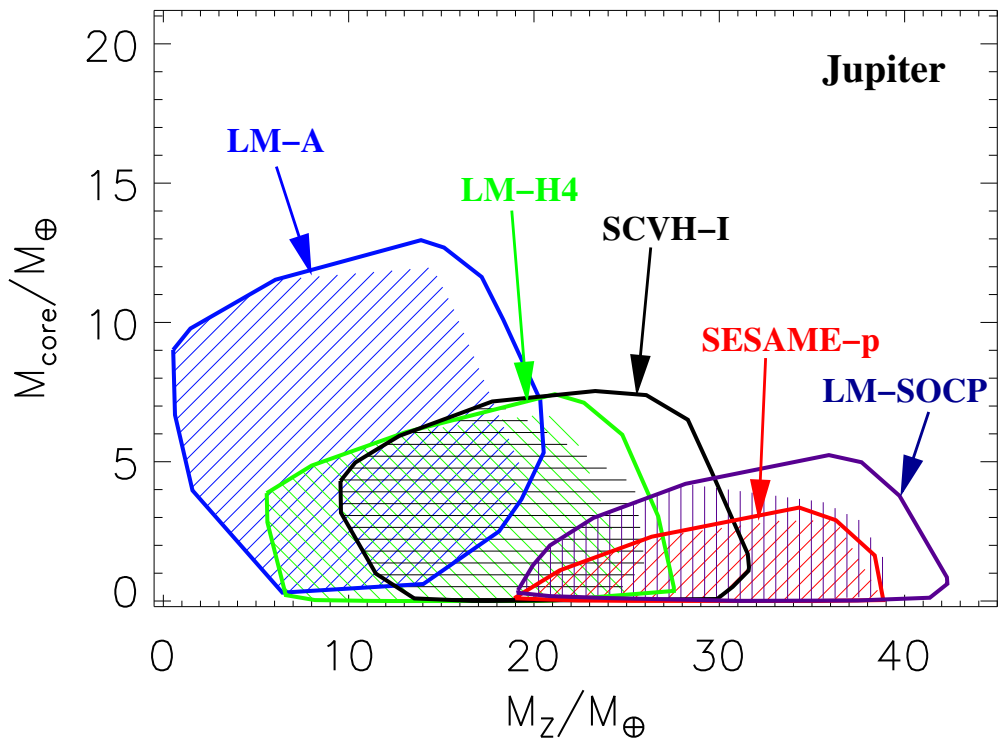


Fig. 9.— Same as Fig. 8 but including an additional 2% uncertainty on the density profile of each EOS (see Eq. 7). The hashed regions represent solutions for which J_4 is within 1σ of the measured value. [See the electronic edition of the Journal for a color version of this figure.]

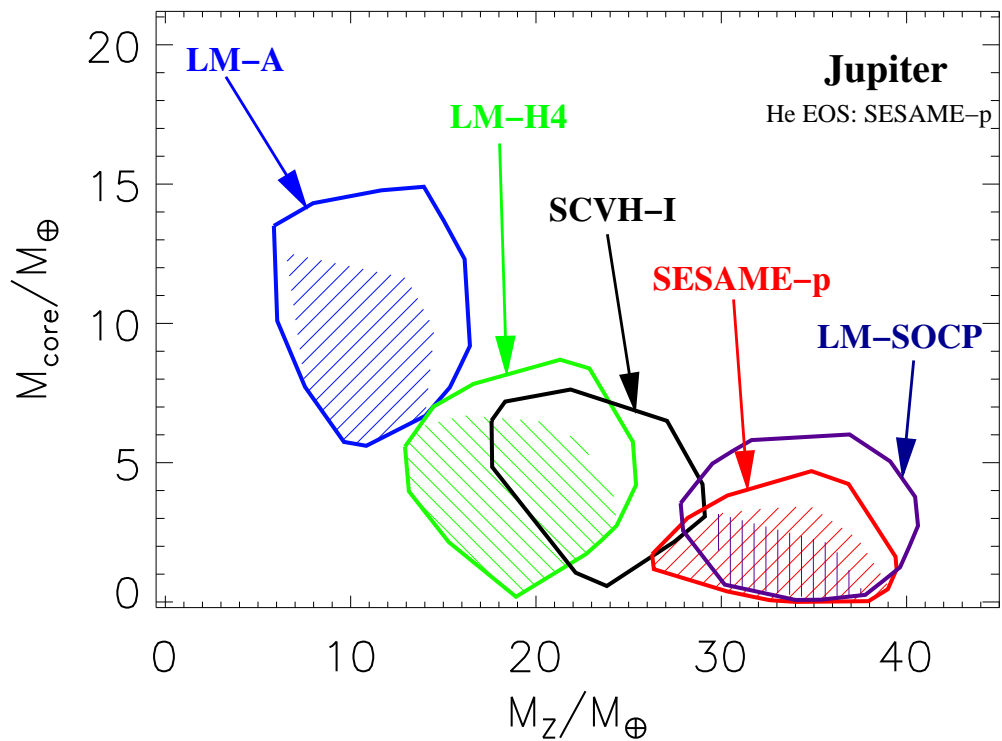


Fig. 10.— Same as Fig. 8 but using the He-SESAME-p EOS for helium instead of the He-SCVH EOS (see text). The hashed regions represent solutions for which J_4 is within 1σ of the measured value. [See the electronic edition of the Journal for a color version of this figure.]

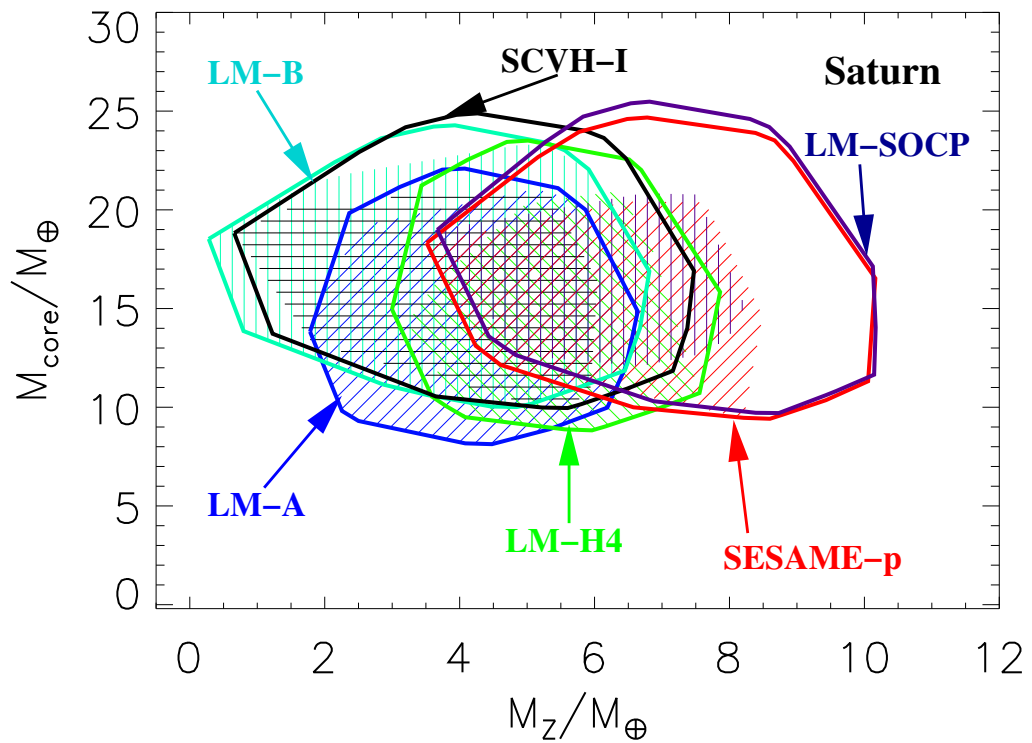


Fig. 11.— Same as Fig. 9 for Saturn. Note the difference of scale for M_{core} and M_z . A 2% uncertainty on each EOS is included (see Eq. 7). The hashed regions represent solutions for which J_4 is within 1σ of the measured value. The total mass of Saturn is $95.147 M_{\oplus}$. [See the electronic edition of the Journal for a color version of this figure.]

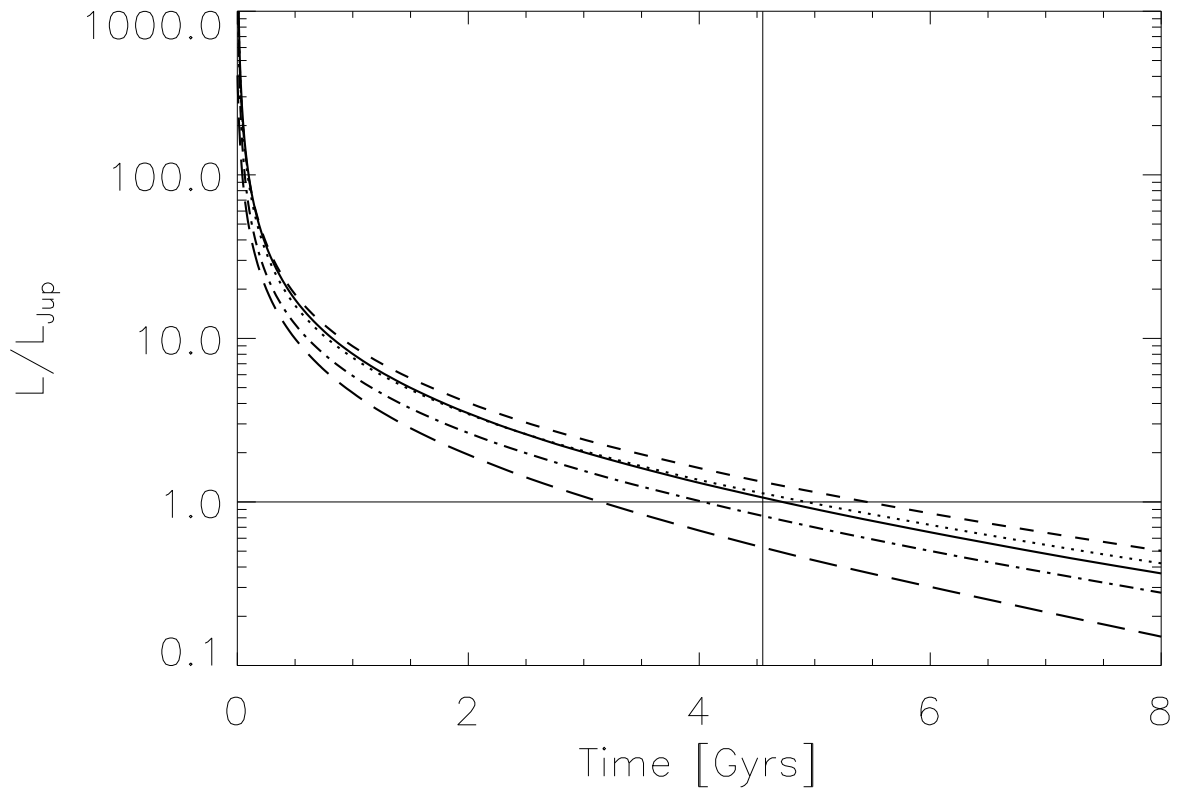


Fig. 12.— Evolution calculations for homogeneous models of Jupiter using various EOS. Jupiter's present luminosity (L_{Jup}) is indicated by the horizontal line. The EOS used are (from left to right) LM-A (long-dashes), LM-H4 (dot-dashed), SCVH-I (plain), LM-SOCP (dotted) and SESAME-p (dashed). The vertical line marks the age of the Solar System, 4.56 Gyr.